

# The elusive crustal resistive boundary beneath the Deccan Volcanic Province and the western Dharwar craton, India

Akkapolu Pratap<sup>1</sup> Bukke Pradeep Naick<sup>2</sup> Kusham<sup>2</sup> Paluri Rama Rao<sup>3</sup> Kasturi Naganjaneyulu<sup>2\*</sup>

<sup>1</sup>**Absolute Imaging International India Limited**  
Noida 201309, India

<sup>2</sup>**Electromagnetic Geophysics, CSIR-National Geophysical Research Institute**  
Hyderabad 500007, India

<sup>3</sup>**Andhra University**  
Visakhapatnam 530003, India

\*Corresponding author, E-mail: kasturi.naganjaneyulu@gmail.com. Fax: 91-40-27171564

## ABSTRACT

The electrical properties of the boundary beneath the Deccan Volcanic Province and the western Dharwar craton are imaged by using the magnetotelluric method. The magnetotelluric study was carried out along a 150km long WNW-ESE profile from Belgaum (in the Deccan Volcanic Province) to Haveri (in the western Dharwar craton). Data from 19 magnetotelluric stations spaced 10-15km apart were used. The dominant regional geo-electric strike direction obtained is N20°E. Two-dimensional (2-D) inversion is done by using the non-linear conjugate gradient scheme for both apparent resistivity and phase. The 2-D resistivity model shows a high electrical resistivity character (>10,000ohm-m) in the western Dharwar craton. Two conductive anomalies are mapped in the crustal region. In the WNW side of the profile, a conductive feature (~200ohm-m) is imaged in the mid-lower crust and, in the central part of the profile another conductive feature is mapped in the lower crust. The robustness of conductive features is tested using linear and non-linear sensitivity analyses. The conductor mapped in the WNW part of the profile is considered as a deep-seated fault representing a boundary or a rift related feature beneath the Deccan Volcanic Province and the western Dharwar craton. A zone of enhanced conductivity (<50ohm-m) at an approximate depth of 10-30km may represent the presence of the rift in the region. This conducting feature on the Western side of the E-W trending Kaladgi Basin can be interpreted as the extension of the Kaladgi Basin further west. A well-correlated geological cross-section is also derived to interpret the resistive features mapped in this study. The electrical resistivity nature of the crust is compared with other regions of the world.

**KEYWORDS** | Crustal structure. Deccan Volcanic Province. Western Dharwar craton. Magnetotellurics. Resistivity.

## INTRODUCTION

In the west-central India, the Deccan Volcanic Province (DVP) is a large basalt province covering an area of about half a million sq. km (Fig. 1). The DVP was formed from the interaction of the mantle plume and the superseding continental lithosphere at ~65Ma ago (White and McKenzie, 1989). The Archaean Dharwar craton (3.4Ga to 2.5Ga) is situated in the southern side of the DVP (Fig. 1). Several sedimentary formations, deformation, igneous activity, and metamorphism characterize the Archaean Dharwar craton (Naqvi and Rogers, 1987). Many researchers have studied the Archaean crustal evolution in the Dharwar craton (Jayananda *et al.*, 2018; Ramakrishnan and Vaidyanadhan, 2010 and references therein). Archaean granite-greenstone belts have received significant attention in early Earth's history, to understand the crust and the emergence of plate tectonics (*e.g.* Condie, 1981; De Wit, 1998). Raase *et al.* (1986) recognized different metamorphic conditions from the northern low-grade to the southern high-grade parts in the Dharwar craton. Recent studies reported arc-related charnockite rocks and ophiolitic assemblages in the Neoproterozoic suprasubduction zone at the southern margin of the Dharwar craton (Clark *et al.*, 2009; Yellappa *et al.*, 2012).

Several studies imaged a conductor wherever there is a boundary of different blocks, faults, and/or shear zones. For example, in the central Indian Tectonic zone, in fault zones like the Purna fault, Gavilgarh fault, and Narmada South fault, the presence of a conductor is reported due to the underplating or fluids (Naganjaneyulu *et al.*, 2010; Naganjaneyulu and Santosh, 2010, 2011 and reference therein). Deep crustal conductors are present beneath the Baltic, Canadian, and Siberian shields, and other regions of the world (Jones, 1992). Low resistivity (200–350ohm-m) is observed at a crustal depth of 20–30km in northern Ontario, Canada (Duncan *et al.*, 1980). The continental lower crust conductance is higher beneath the southern side of the Baltic shield and the eastern side of the Siberian shield. Jiracek *et al.* (1979) compared the interpretation of four different rifts (East African rift, Rio Grande rift, Baikal rift, and Midcontinent rift) and concluded that a zone of enhanced conductivity (<50ohm-m) at an approximate depth of 10–30km is a common feature in those regions. In the present study, the electrical resistivity structure of the crust and uppermost mantle region beneath the DVP and the western Dharwar craton is imaged using the magnetotelluric (MT) method, a geophysical technique for imaging the electrical resistivity structure of the crust and upper mantle region (Brasse *et al.*, 2009; Bologna *et al.*, 2017; Kusham *et al.* 2018, 2019, 2021a, b; Naganjaneyulu and Harinarayana, 2004; Naganjaneyulu and Santosh, 2010a, b; Naganjaneyulu and Santosh, 2011; Nagarjuna *et al.*, 2017; Pina-Varas *et al.*, 2014; Pratap *et al.*, 2018;

Sarafian *et al.*, 2018). Magnetotellurics have been thoroughly employed to describe fault and shear zones (Adetunji *et al.*, 2015; Naganjaneyulu *et al.*, 2010a, b; Rao *et al.*, 2014; Wu *et al.*, 2002).

Various geological and geophysical studies have been carried out in the Dharwar craton and surroundings. These studies mapped the crustal and lithospheric structure and lithospheric thickness beneath the Dharwar craton. Seismology studies of artificial and natural source (surface waves, body waves, absolute velocity tomography, and receiver functions) show significant variations in the crustal thickness and bulk  $V_p/V_s$  velocity in the south Indian shield (Julia *et al.*, 2009; Rai *et al.*, 2003; Ravi Kumar *et al.*, 2001). A deep seismic sounding study along the 600km long Kavali-Udipi profile (Fig. 1) imaged a few deep-rooted faults that extended up to the Moho boundary. Kaila *et al.* (1979) estimated a crustal thickness of approximately 41km in the western Dharwar craton. Sarkar *et al.* (2001) interpreted a thickness of 23km for the upper crust and a Moho depth at about 37–40km. From the spectral analysis of aeromagnetic anomaly maps, the crustal thickness inferred in the Dharwar craton is 36km (Rajaram and Anand, 2003). According to teleseismic studies, the crustal thickness in the northern, central, and southern parts of the western Dharwar craton is 42–46km, 38–42km, and 48–52km respectively (Borah *et al.*, 2014b). Using the joint inversion of receiver function and Rayleigh wave group velocity analysis, the Moho depth determined is ~40km beneath the mid-Archaean western Dharwar craton (Saikia *et al.*, 2017).

Numerous regions in the DVP show variations in heat flow in the range of 34–49mW/m<sup>2</sup> (Roy *et al.*, 2008; Roy and Rao, 2000). Based on surface heat flow values, it is estimated that the lithosphere is <120km thick in the DVP, whereas it is >140km thick in the western Dharwar craton (Negi *et al.*, 1986). The heat flow values are plotted on the map (Fig. 1; Gupta *et al.*, 1991; Roy *et al.*, 2008; Roy and Rao, 2000). Kumar *et al.* (2013), based on the assumption of the isostatic equilibrium gravity model and constrained by several geophysical data sets, estimated that in the Dharwar craton the crustal thickness is about 40km, and the lithospheric thickness is 150–180km.

A few magnetotelluric studies have been carried out in the Dharwar craton and the DVP (Fig. 1). The results from the central Indian tectonic zone are considered to understand the nature of faults/shears/boundaries. A few studies observed that the Deccan basalts overlying the granitic upper crust were about 500m thick. A mid-crustal conductor was imaged at a depth of 10–20km (Gokarn *et al.*, 1992). Two conductive zones are delineated that correspond to the Khandwa lineament and the Burhanpur tear. A prism-shaped body in the Satpura horst region is

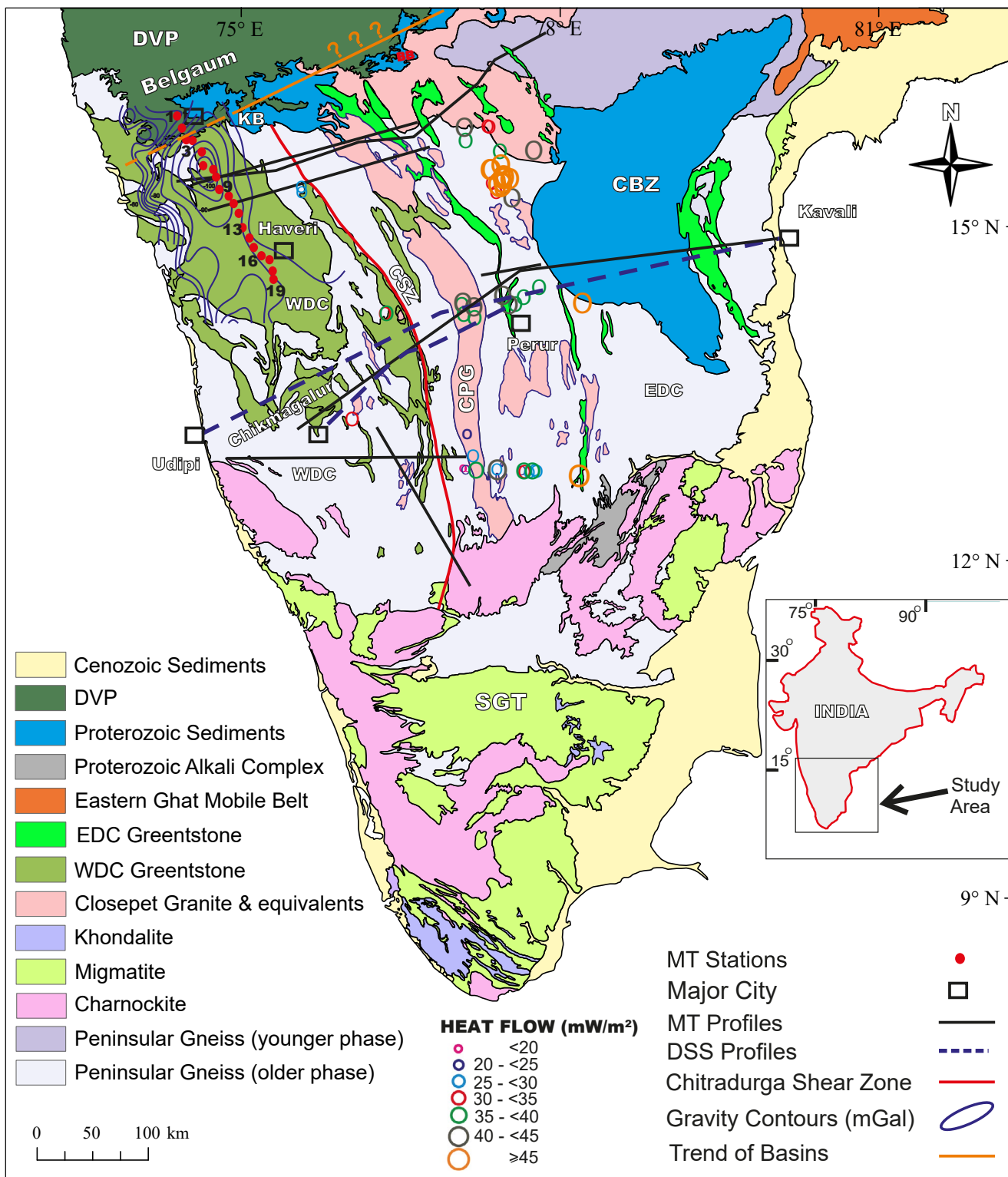


**FIGURE 1.** A simplified geological map of the southern Indian shield region showing the locations of magnetotelluric stations (red circles). Black lines represent previous magnetotelluric profiles, and dashed blue lines represent Deep Seismic Sounding (DSS) profiles. The orange line shows the trend of the basins. The red NW-SE line shows the Chitradurga Shear zone. Tectonic elements include DVP: Deccan Volcanic Province, CSZ: Chitradurga Shear Zone, KB: Kaladgi Basin, BB: Bhima Basin, CB: Cuddapah Basin, CPG: Closepet Granite, WDC: Western Dharwar Craton, EDC: Eastern Dharwar Craton, SGT: Southern Granulite Terrain. Heat flow values are from Gupta et al., 1991; Roy et al., 2008; Roy and Rao, 2000.

observed at depths between 3 to 14km with a resistivity of 20ohm-m. The body has a lateral extent of 8km at its top and 40km at the bottom in the N–S direction. It is well correlated with the other geophysical results in the Satpura and Tapti regions (Rao and Singh, 1995). In the western Dharwar craton, only few studies are available that coincide with our study region. Three magnetotelluric profiles that are perpendicular to the present study profile (black lines in Figure 1) image several low resistivity features at various depths (Gokarn *et al.*, 2004; Kusham *et al.* 2018, 2019). A recent MT study in the southern part of the present study maps a conductor at a depth range of 20–50km, and the conductor shows a good match with the Chitradurga shear zone and Biligiri Rangan charnockite massif (Pratap *et al.*, 2018).

The continental lithosphere imaged by the magnetotelluric method helps to reveal its deformation, structure, and preservation (Jones, 1999; Davis *et al.*, 2003; Ferguson *et al.*, 2012 and references therein). Many potential sources, which enhance lithospheric conductivity, can be interpreted based on the local geological and geophysical conditions of the area (Korja, 2007; Schwarz, 1990; Selway, 2014). In the lithosphere, the enhanced conductivity sources are water, graphite, partial melt, hydrogen, and temperature (Constable, 2006; Ducea and Park 2000; Hirth *et al.*, 2000; Jones, 1999; Karato, 1990; Korja, 2007; Mibe *et al.*, 1998; Muller *et al.*, 2009; Selway, 2014; Yoshino *et al.*, 2008 and references therein). The present study is based on a ~150km long WNW–ESE magnetotelluric profile that passes through the DVP region and extends into the western Dharwar craton (Fig. 1). This study aims to delineate the electrical resistivity nature of the boundary beneath the DVP and the western Dharwar craton and to find out the possible causes of enhanced conductivity in the crust, if any.

## GEOLOGICAL AND TECTONIC FRAMEWORK

A geological and tectonic map of the southern Indian shield with the location of the MT stations is shown in Figure 1. The Archaean Dharwar craton, also known as the Karnataka craton, is a widely studied terrain of the southern Indian shield. It presents an Archaean cratonic core of Tonalite-Trondhjemite-Granodiorite (TTG) gneisses intruded by younger granites in the association through the basement accumulation of linear schist belts (Anil Kumar *et al.*, 1996; Bhaskar Rao and Naqvi, 1978; Hegde and Chavadi, 2009; Swami Nath and Ramakrishnan, 1981 and references therein). The western Dharwar craton hosts several gold deposits in the mafic volcanic schist belts, mainly in the Chitradurga belt. The western Dharwar craton is bounded on the west by the Arabian sea, on the north by the DVP, on the south by the southern granulite terrain and, on the East it is separated from the eastern Dharwar craton

by the Chitradurga shear zone. In the Dharwar craton, the schist and greenstone belts are present with sedimentary associations. The schist belts include chemical sediments and extensive basalts with subordinate fine clastic rocks, in assured areas through basaltic conglomerated and clastics shallow water that is rippled-bedded quartzites and shelf-sedimented. Archaean rock unit formations occurred in this terrain between 3.6Ga and 2.5Ga (Radhakrishna and Naqvi, 1986). The intensity of metamorphism gradually increases from greenschist facies to amphibolite facies from north to south, and the structural trends were generally N–S to NNW. The western Dharwar craton has two distinct ages; 2.7–3.0Ga on the northern side and 3.0–3.4Ga on the southern side. The core of the western Dharwar craton contains the oldest rocks of the south Indian shield, representing the mid-Archaean greenstone belts (Raase *et al.*, 1986). The southern part of the western Dharwar craton contains an older (3.36Ga) crust in the form of greenstone belts (Peucat *et al.*, 1995; Taylor *et al.*, 1984). Geologically, the western Dharwar craton is dominated by TTG-type gneisses with an interlayered Sargur Group greenstones that are unconformably overlain by younger Dharwar supergroup greenstones. The Sargur group is dominated by Komatite-basalts. It has a predominance of siliciclastic and chemical sediments. Whole-rock geochemical, petrographic, and Nd isotopic studies reported that the Komatites magmas were derived from melts originated in the upper mantle at different depths (Jayananda *et al.*, 2008, 2013). In the Dharwar supergroup, a second magmatic episode corresponds to felsic-mafic rocks of 2.6–2.8Ga. A third magmatic episode corresponds to Proterozoic dyke mafic swarms of three main periods *i.e.* 2.4, 2.0–2.2 and 1.6Ga. Chadwick *et al.* (1997) based on isotopic age data suggested that volcanic rocks have erupted in the period 2.75–2.65Ga, whereas granite emplacement took place in the period 2.75–2.55Ga.

The southern Indian shield consists of several tectonic blocks separated by a complex set of faults and shear zones. These tectonic blocks comprise Archaean granitoid terranes of amphibolite and granulite facies. The DVP marked the northern edge of the western Dharwar craton. Earlier studies suggested that the deep crust beneath the DVP contains pockets of fluid reservoirs generated by the transfer of fluids from plume-related mantle-derived magmas associated with the Deccan volcanism. Numerous types of basalts have been observed in the DVP indicating the diverse crystallisation and differentiation of the different magma types during transport and in magma chambers. Based on petrographic and mineralogical data from numerous sections, it has been inferred that minerals such as olivine, clinopyroxenes, plagioclase, and opaque oxides including spinels show considerable variations depending upon the tholeiitic or alkaline character of the host magma and its degree of evolution (Krishnamurthy, 2020).

The Kaladgi Basin (KB) and Bhima Basin (BB) are intracratonic basins of Proterozoic age. These basins are overlain by the Deccan Flood Basalt (DFB) and underlain by the Archean Dharwar craton (Fig. 1). The trend of the KB and BB is also shown in Figure 1. The E–W trending normal faults with external stress regime controls the evolution of the KB (Jayaprakash, 2007). The NE–SW trending BB dominantly consists of limestone formations. It is situated NW of the Cuddapah Basin and NE of the KB. BB has several faulted contacts with the eastern Dharwar Craton. The BB appears to be a pull-apart basin exposed in narrow strips arranged in an en echelon pattern (Dey, 2015). According to Klein (1995), the intracratonic basins are generally underlain by failed rifts. Due to very limited information available on the KB and BB, whether or not these basins are also underlain by failed rifts remains debated. On the basis of gravity lows, Krishna Brahmam and Negi (1973) suggested the presence of two rift valleys underlying the Deccan Trap volcanics. According to these authors, the sediments of the KB and BB were deposited in two rift valleys. According to Ramakrishna and Chayanulu (1988), the observed gravity low is due to normal depression (*i.e.* a basin filled with sediments), not due to any major fracture zone below. Reactivation of weaker zones or pre-existing lineaments, upwelling of hot mantle material, or hotspots may initiate rifting in the crust (Miall, 1984). Another study proposed that the extension and rifting occur due to the instability induced by the sinking of the lithosphere owing to the overlying structure (Fourel *et al.*, 2013).

## METHODOLOGY

The magnetotelluric (MT) method is an efficient tool for exploring the Earth at deep crustal levels. This method provides electrical structures over various depths from shallower levels to as deep as tens to hundreds of kilometers. The MT data obtained in this study along a traverse from Belgaum to Haveri are shown in Figure 1. In the present study, data are recorded by using the Lviv LEMI-418 and LEMI-420 magnetotelluric systems of the Lviv Centre at the Institute for Space Research, Ukraine. The LEMI-418 system is a broadband magnetotelluric data acquisition station. It records the Earth's electric and magnetic field variations. It provides measurements in different sampling ranges: high-frequency range (640Hz or 640sps), medium-frequency range (40Hz or 40sps), and low-frequency range (1Hz or 1sps). For ranges <1Hz the long-period magnetotelluric station LEMI-420 is also used. The telluric field measurements are made with non-polarized electrodes (Cu/CuSO<sub>4</sub>), and the magnetic field measurements are made with an induction coil (high and medium frequency ranges) and fluxgate magnetometers (low frequency). The electrode separation is about 100m.

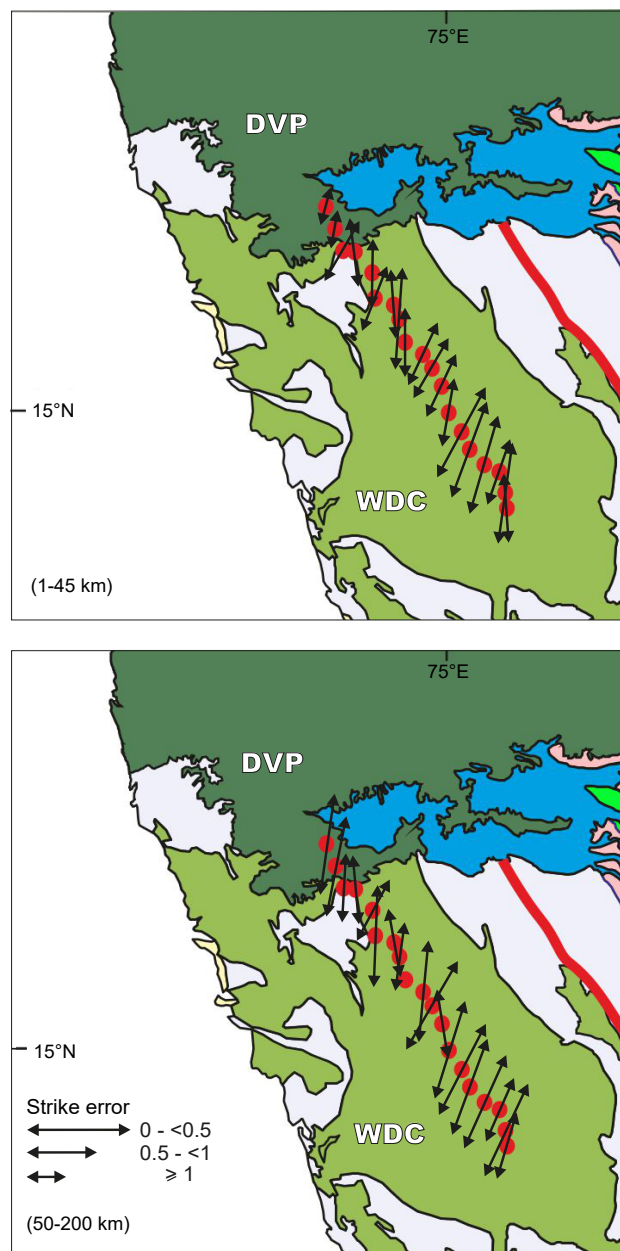


**FIGURE 2.** Geo-electric strike direction derived from the magnetotelluric tensor decomposition method for different depth bands: A) crustal (1–45km), B) lithospheric mantle (50–200km).

The data are collected at 19 stations along a 150km long profile. For each station, the recording time varies between 3–15 days. Time series processing is carried out using the robust processing code (Chave and Thomson, 2004) in the period range of 0.01–10,000s to obtain the transfer functions (resistivity and phase). Before obtaining the 2-D model, the data are subject to tensor decomposition (McNeice and Jones, 2001) and checked for static shift corrections (see Jones, 1988 for a review). The McNeice and Jones (2001)'s tensor decomposition method that depends on Groom and

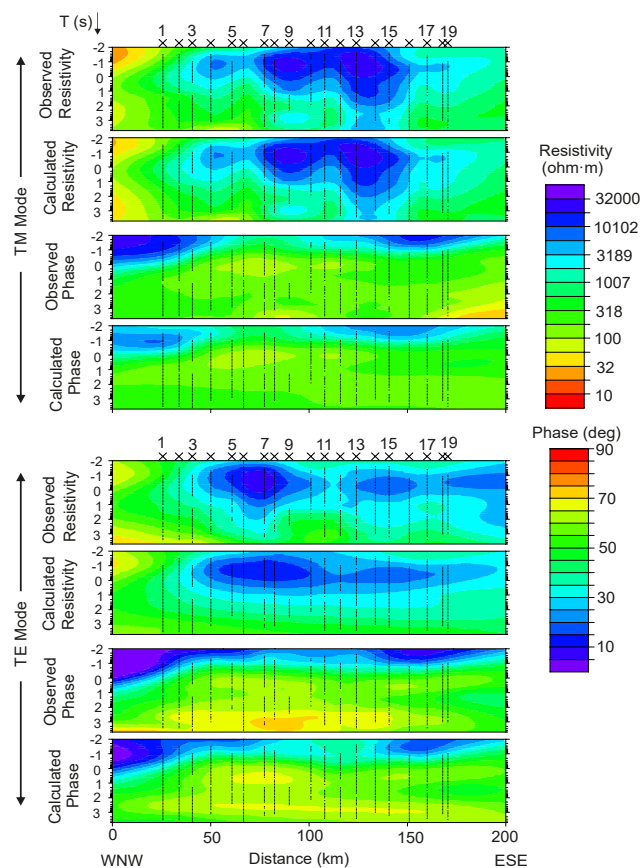


**FIGURE 3.** Apparent resistivity and phase pseudo-sections of transverse magnetic (TM) mode (upper panel) and transverse electric (TE) mode (lower panel) for the resistivity model. Each panel shows the observed and calculated responses of the 2-D resistivity model.

Bailey (1989)'s galvanic distortion is used for the analysis. For strike evaluation at crustal and lithospheric mantle depths, the length of the arrows is scaled by a standard Root Mean Square (RMS) error (Fig. 2). The strike results for the crustal (1–45km) and lithospheric mantle (50–200km) depths are shown in Figure 2. The geo-electrical strike direction is derived from various trials followed by different depth bands and impedance errors. The geo-electric strike estimation, shown in Figure 2, is based on an impedance error floor of 5% (equivalent to 2.86° in phase and 10.25% in resistivity). Generally, a low RMS error of less than 2-3 indicates 2-D assumption is valid (see Dong *et al.*, 2015). The dominant geo-electric strike estimation is N20°E and the stations are projected to a N110°E striking profile accordingly to obtain the 2-D model. So we rotated the data to N20°E. We have data from a profile further south of the present study profile (manuscript under preparation) that show a strike direction N14°E. In this study, a non-linear conjugate gradient inversion algorithm, proposed by Rodi and Mackie (2001, 2012) is used for the 2-D inversion of the data. A mesh of 67 horizontal and 137 vertical elements with 100ohm-m resistivity values is used to get the initial

2-D model. The apparent resistivity error floor is set to 15% and the phase error floor is set to 1.45° (equivalent to 5%) for both Transverse Electric (TE) mode in which the electric field is parallel to the geoelectric strike; and Transverse Magnetic (TM) mode in which electric field is perpendicular to the geoelectric strike. The relatively high error floor for apparent resistivity data compared to phase data helps to overcome possible static shift effects in the data, if any (Dehkordi *et al.*, 2019; Naganjaneyulu, 2010; Naganjaneyulu and Santosh, 2012).

## RESULTS

The TE and TM modes apparent resistivity and phase pseudo-sections of the present profile are shown in Figure 3. The apparent resistivity response is dominated by the high resistivity value (>10,000ohm-m) beneath the central part of the profile in the shortest period range (0.01–100s). At mid-crustal depths, a low resistive (<1,000ohm-m) response was observed in the WNW and ESE parts of the profile. The observed data (rotated to 20°) and computed responses for the resistivity model at different magnetotelluric stations are shown in Figure 4. The final model RMS error is 2.5. The 2-D inversion model and sensitivity analysis (linear and non-linear) are shown in Figures 5, 6 and 7 respectively. The model shows the crust is highly resistive (>10,000ohm-m), and this resistive nature extends to a depth of about 50km throughout the profile (Fig. 5A). Two conductive features (A and B) are imaged in the crust (Fig. 5A). On the WNW side of the profile, conductive feature 'A' is identified in the mid-lower crust with a low resistivity value (<200ohm-m). Another low resistive feature 'B' is mapped in the lower crust of the central part of the profile. The linear sensitivity analysis with high sensitivity values (more than 1) supports the presence of a conductive feature 'A' (Fig. 6). A conductive feature 'B' is supported by sensitivity values of more than 0.1. The robustness of these features is also tested by inserting the resistive features in the place of conductive features and carrying out forward modelling. In this analysis, conductive features are replaced with a 3,000ohm-m resistivity value. The deviations in the calculated response for conductor 'A' confirm that the conductive feature mapped in the model is robust (Fig. 7). An example of non-linear sensitivity analysis at station number 2 above conductor 'A' is shown in Figure 7. During the sensitivity analysis, it was noticed that the resistivity value ~1,000ohm-m was necessary for conductor 'B'. Acquisition of additional data in this region to provide better constraints for the subsurface 3-D inversion model is pending.

## DISCUSSION

The region underneath the western Dharwar craton and the adjacent DVP has been investigated using data from

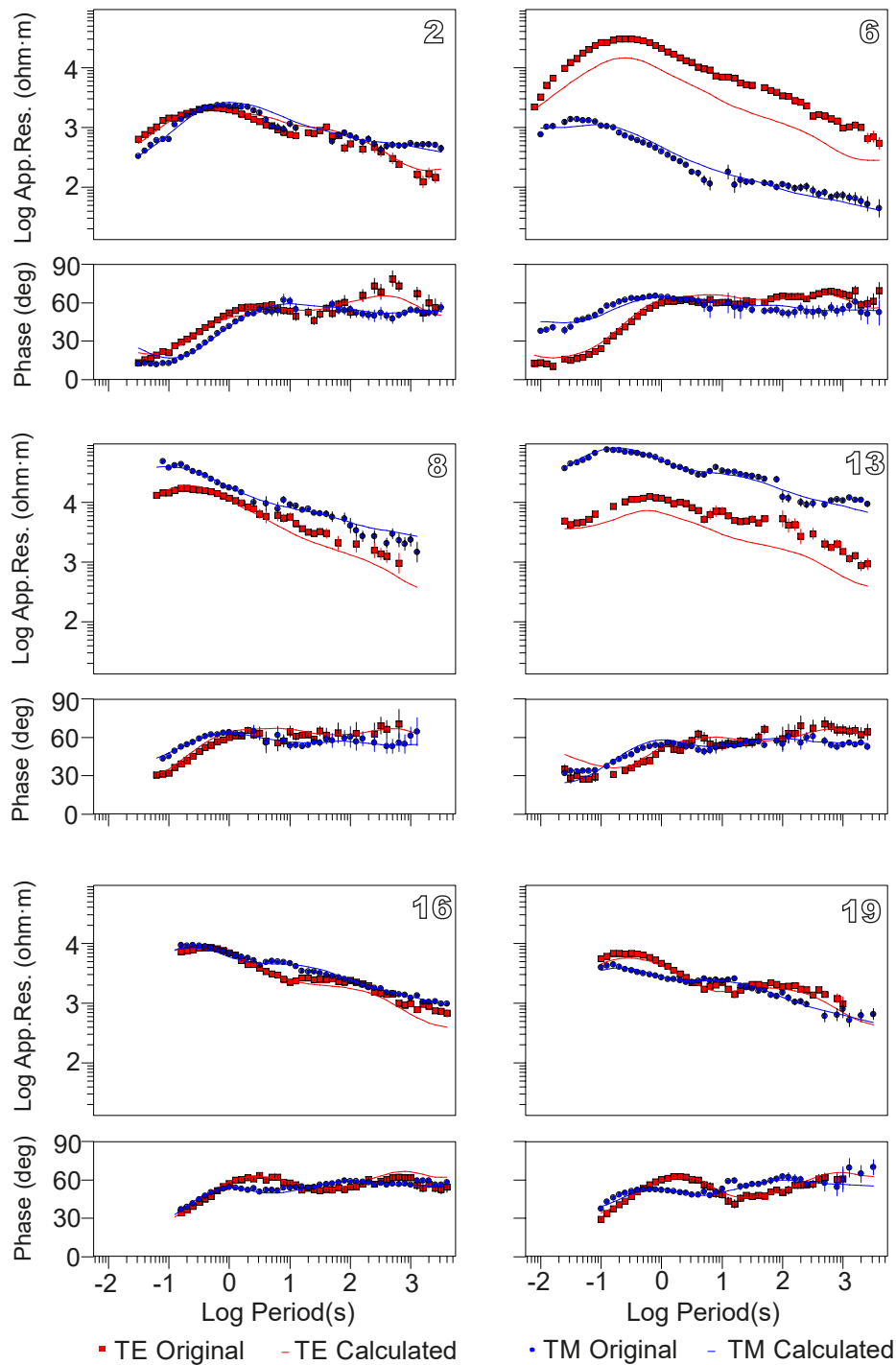


**FIGURE 4.** Fit of the observed data and computed responses for some MT stations for the lithospheric resistivity model.

19 magnetotelluric stations. The model derived from the WNW–ESE profile is utilized to map the geo-electrical structure of the crust. The results presented in this study show a significant correlation with previous geological and geophysical studies in a similar geological domain. The resistivity of the stable lower crust varies from about

10 to greater than 10,000ohm·m worldwide (Korja and Hjelt, 1993; Jones, 1992; Jones *et al.*, 2005; Haak and Hutton, 1986; Selway *et al.*, 2011). In the deep crust, high electrical conductivity can be possibly invoked by partial melt (Hermance, 1979; Schilling *et al.*, 1997), thin graphite films (Glover and Vine, 1992), and the presence of fluids

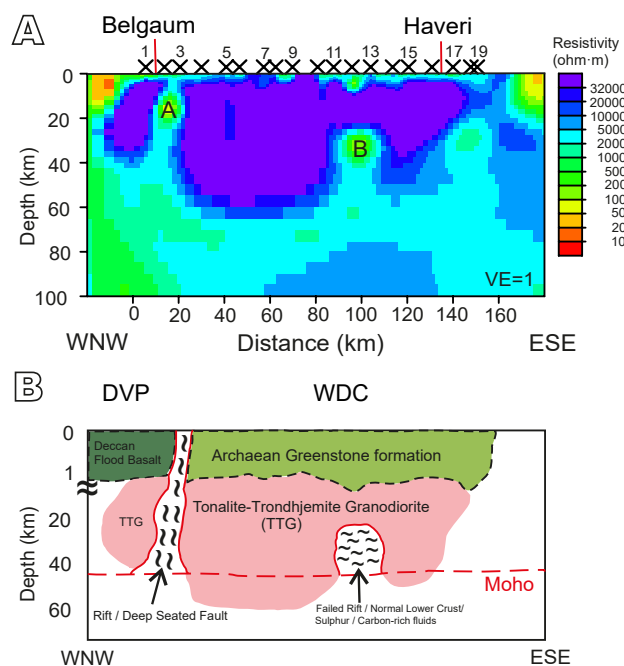


**FIGURE 5.** A) Two-dimensional (2-D) resistivity model along the profile; B) Geological cross-section along the profile.

(Hyndman and Shearer, 1989). Partial melting could be the reason for very low resistivity in regions where the lower crustal temperature is 650 or 700°C. In the region of the present study partial melting is ruled out given the reduced heat flow values (usually <math><50\text{mW/m}^2</math>) observed.

A low resistive feature is detected beneath the DVP and the Archaean western Dharwar craton on the northern side of the profile (conductor 'A' beneath stations 2 and 3) (Fig. 5A). The conductor 'A' is present at the margin of the large-scale greenstone formations. This conductive feature (~200ohm-m) is at a depth of approximately 10km, and it extends down to a depth of about 25km. A few geological studies inferred an E–W trend of the archaean basins of the western Dharwar supergroup, implying that a volcanic

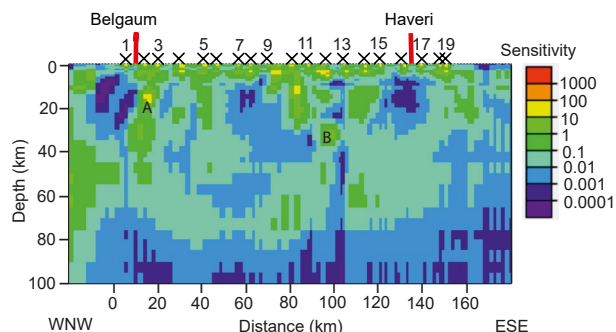


**FIGURE 6.** The linear sensitivity matrix for the Belgaum-Haveri profile shows how the small change of the logarithm of resistivity in each model cell influence the data.

arc related to the southern subduction scenario is buried underneath the DVP (Chadwick *et al.*, 1997; Newton, 1990; Srinivasan and Naha, 1993). Based on palaeomagnetic and geochemical data, Hasnain and Qureshy (1971) stated that a Cretaceous dyke is present near the Chitradurga region, Karnataka, and correlated it with Deccan volcanism. Such dykes may therefore create an expression of crustal extension and rifting. Thus, conductor 'A' can be interpreted in terms of a deep-seated fault or a rift related feature beneath the DVP and the western Dharwar craton. A similar localized conductive feature (~30ohm-m) is mapped in the upper crust beneath the Central Metasedimentary Boundary Belt Zone (CMBBZ) of the Proterozoic Grenville Province (Adetunji *et al.*, 2015). CMBBZ is a shear zone that separates the Central Metasedimentary Belt (CMB) and Central Gneiss Belt (CGB). The CMB lies to the southeast of the CGB. The shear zone (CMBBZ) indicates the thrusting of the CMB northwestwardly against the CGB (Davidson, 1998; Easton, 1992). Another similar conductive anomaly (<math><50\text{ohm-m}</math>) is imaged in western Burkina Faso in the upper crust beneath the Hounde greenstone belt. The less-dense volcanic lithologies of the Hounde greenstone belt correlates well with the mapped conductive anomaly in terms of depth and width and is interpreted in terms of the presence of graphite in the sequence (Pape *et al.*, 2017). Contrary to this, in the North American Central Plains (NACP), an anomalous conductive feature (~10ohm-m), mapped in the depth range of 5–10km, with a lateral extension of about 20km, is associated to the occurrence of sulphides rather than graphitic metasediments (Jones, 1993).

In the central part of the profile, another conductive feature 'B' is identified in the depth range of about 30–45km. The conductor 'B' is related to a gravity high (-80 to -90mGal), as shown by the contours in Figure 1 (Subrahmanyam and Verma, 1982). The conductive feature 'B' underestimates the resistivity value, the feature is robust for the resistivity value of ~1000ohm-m. This feature can be explained by several processes, such as failed rift, underplated mafic magma complex, brittle-ductile transition (rheological boundary), sulphur and carbon-rich fluids etc. A failed rift forms when a rifting process is sustained only for a short span of time. A failed rift can result in this type of feature in the lower crust. The rheological boundary could act as an impermeable barrier to the upward flow of fluids trapped in the lower crust. These trapped fluids can deposit sulphur or carbon-rich fluids in the lower crust. Pan-African Orogenesis (deformation and metamorphism) also results in high content of sulphide in the lower crust (Miensoopust *et al.*, 2011).

Bruhn *et al.* (2004) identified and interpreted the lower crustal conductor in terms of sulphur and carbon-rich fluids. The gold mineralization in the Hutti and Kolar schist belts provides strong indications of carbon and sulphur-rich

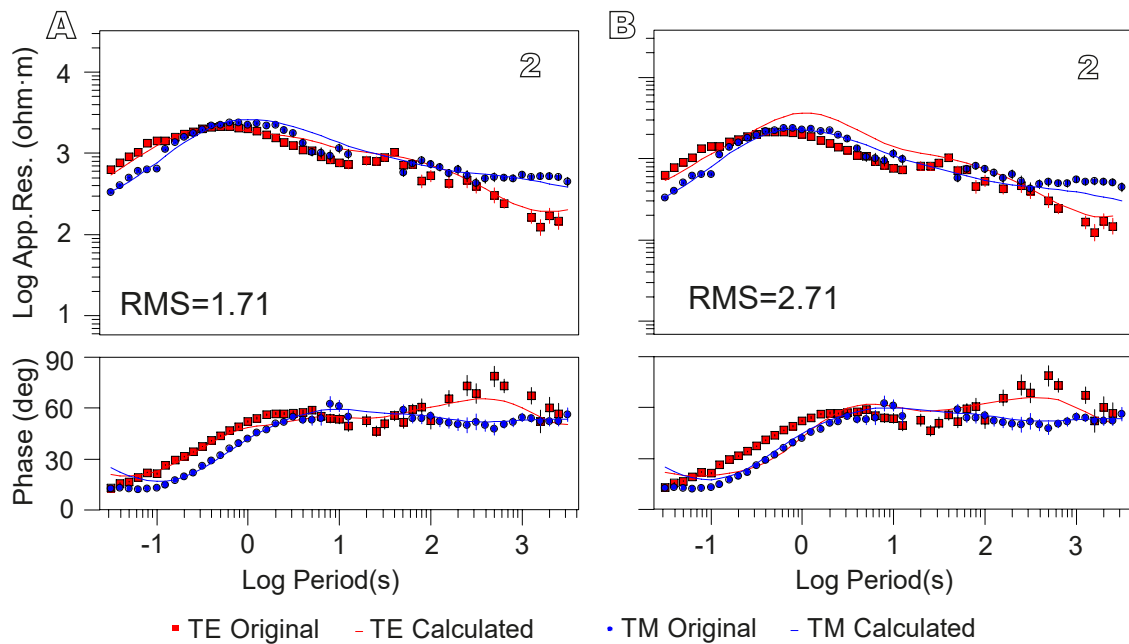


**FIGURE 7.** Comparison of TE and TM mode apparent resistivity and phase responses between an A) original model with conductor and B) an alternative model without conductor (3,000ohm·m) at station 2 above the conductor.

fluids in the lower crust, which act as the channels for such mineralization (Gokarn *et al.*, 2004). The conductive lower crust (~50ohm·m) has been mapped in stable plate interiors like the Kaapvaal and Zimbabwe cratons in South Africa (Khoza *et al.*, 2013; Miensoopust *et al.*, 2011; Muller *et al.*, 2009) and the northeastern Rae craton region in Canada (Evans *et al.*, 2005). An anomalously low conductive feature (~10ohm·m) is mapped in the lower crust beneath the Hearne craton, northern Canada (Jones *et al.*, 2005). The cause of lower crustal conductivity is due to the ionic conduction (in saline water and partial melt) and electronic conduction (in graphite, sulphide, and iron oxide metasediments or in carbon grain boundary films) (*e.g.* Duba *et al.*, 1994; Jones, 1992; Wannamaker, 1997; Yardley and Valley, 1997). Partial melt is generally ruled out for the old and cold cratonic lower crust. The petrological evidences are against the existence of free fluid in Precambrian regions. In the case of the Hearne craton (northern Canada), the authors considered the tectonic emplacement of metasediments deep into the crust during an orogenic event as the likely cause of lower crustal conductivity. It is thus inferred here that feature 'B' is caused by either sulphur deposited in the form of pyrite or the presence of sulphur and carbon-rich fluids, which may have risen through the fractured parts of the upper crust. Kariya and Shankland (1983) suggest that the lower crustal material yield the resistivities of mafic dry rocks around 1000ohm·m at 800°C temperature. Haak and Hutton (1986) considered the resistivity of the Continental Lower Crust (CLC) normally lie in the range of 100–1000ohm·m. The values above and below this range

are considered as anomalously high and anomalously low respectively. The age of the shield region also affects the resistivity of the CLC. The CLC becomes more resistive with age (Keller, 1989b; Jones, 1981b). In the present study, the conductive feature 'B' mapped in the lower crust lies in a similar resistivity range. This study also shows the extremely resistive nature (>10,000ohm·m) of the upper crust all along the profile (Fig. 5A). This suggests the presence of the TTG crust. The TTG crust is overlain by the Archaean greenstone formation in the western Dharwar craton (Fig. 5A). Moho depth is plotted from the result of previous geophysical studies in the region (Borah *et al.*, 2014b; Saikia *et al.*, 2017). The final resistivity model is correlated with the geological cross-section for the interpretation of the features mapped in the present study (Fig. 5B).

## CONCLUSIONS

A magnetotelluric study is carried out in the Deccan Volcanic Province (DVP) and western Dharwar craton to know the crustal structure and tectonics (faults, rifts, dykes, etc.) underneath them. The ENE–WSW trending 600km long Kavali-Udipi profile (DSS sounding), adjacent to the present study profile, maps several deep-seated faults up to the depth of about 50km. The deep-seated faults serve as a reliable indicator of boundaries, shear zones, rifts, and dykes present in the region. The formation of basins and intraplate tectonism is typically linked to the formation or break-up

of a supercontinent. The Kaladgi Basin (KB) and Bhima Basin (BB) are positioned over the eroded edges of the schist belts and the Archaean complex of the Dharwar craton. The present study profile is located near the western edge of the KB. Flood basalts and dyke swarms (basic and ultrabasic) indicate the signature of crustal-scale extension and rifting at various stages during the Proterozoic. Detection of anomalies beneath the DVP and western Dharwar craton is the main finding of this study. The resistivity distributions in the upper 1000m depth beneath the DVP and the western Dharwar craton are correlated with the Deccan flood basalt and the Archaean greenstone formation, respectively. This study shows the extremely resistive nature (>10,000ohm-m) of the upper crust all along the profile. This suggests the presence of the Tonalite-Trondjemite-Granodiorite (TTG) crust. In the central and ESE sides of the profile, the mid-lower crust shows a less resistive nature, which represents the normal lower crust or sulphur and carbon-rich fluids. The conductive nature beneath stations 2 and 3 gives a clue to the presence of a deep-seated fault representing a boundary or a rift near the DVP and the western Dharwar craton. The extension of the E–W trending Kaladgi Basin (KB) to further west could be the cause. The study also indicates the presence of sulphur and carbon-rich fluids in the region.

## ACKNOWLEDGMENTS

We thank the Editorial committee for handling this manuscript. We appreciate the critical comments, suggestions, and recommendations of anonymous reviewers, which helped to improve the earlier version of the manuscript. We are grateful to Prof. Alan Jones for providing a multisite, multifrequency MT tensor decomposition code. We express our sincere gratitude to Dr. S.S. Rai and Dr. R.K. Chadha for providing encouragement and support. We acknowledge Dr. B. Sreenivas for a fruitful discussion on the geological prospects of the study area. The authors thank Director, CSIR – NGRI, for his permission to publish this work.

## REFERENCES

- Adetunji, A.Q., Ferguson, I.J., Jones, A.G., 2015. Imaging the mantle lithosphere of the Precambrian Grenville: large-scale electrical resistivity structures. *Geophysical Journal International*, 201, 1038-1059.
- Bhaskar Rao, Y.J., Naqvi, S.M., 1978. Geochemistry of Metavolcanics from the Bababudan Schist Belt; A Late Archaean/Early Proterozoic Volcano-Sedimentary Pile from India. *Developments in Precambrian Geology*, 1, 325-341.
- Bologna, M.S., Egbert, G.D., Padilha, A.L., Pádua, M.B., Vitorello, I., 2017. 3-D inversion of complex magnetotelluric data from an Archean-Proterozoic terrain in northeastern São Francisco Craton, Brazil. *Geophysical Journal International*, 210, 1545-1559. DOI: <https://doi.org/10.1093/gji/ggx261>
- Borah, K., Rai, S.S., Prakasam, K.S., Gupta, S., Priestley, K., Gaur, V.K., 2014b. Seismic imaging of crust beneath the Dharwar craton, India, from ambient noise and teleseismic receiver function modelling. *Geophysical Journal International*, 197, 748-767.
- Brasse, H., Kapinos, G., Li, Y., Mütschard, L., Eydam, D., 2009. Structural electrical anisotropy in the crust at the south-central Chilean continental margin as inferred from geomagnetic transfer functions. *Physics of the Earth and Planetary Interiors*, 173, 7-16. DOI: 10.1016/j.pepi.2008.10.017
- Bruhn, D., Raab, S., Schilling, F., 2004. Electrical Resistivity of Dehydrating Serpentine, *Eos Trans. AGU*, 85(47), Fall Meeting, Abstract T41B-1176.
- Chadwick, B., Vasudev, V.N., Hegde, G.V., 1997. The Dharwar craton, southern India, and its Late Archean plate tectonic setting: current interpretations and controversies. *Proceedings of the Indian Academy of Sciences (Earth Planetary Science)*, 106, 249-258.
- Chave, A.D., Thomson, D.J., 2004. Bounded influence magnetotelluric response function estimation. *Geophysical Journal International*, 157, 988-1006.
- Clark, C., Collins, A.S., Timms, N.E., Kinny, P.D., Chetty, T.R.K., Santosh, M., 2009. SHRIMP U-Pb age constraints on magmatism and high-grade metamorphism in the Salem Block, southern India. *Gondwana Research*, 16, 27-36.
- Condie, K.C., 1981. *Archean Greenstone Belts*. Amsterdam, Elsevier, 434pp.
- Constable, S.C., 2006. SEO3: a new model of olivine electrical conductivity. *Geophysical Journal International*, 166, 435-437.
- Davis, W.J., Jones, A.G., Bleeker, W., Grutter, H., 2003. Lithosphere development in the Slave craton: a linked crustal and mantle perspective. *Lithos*, 71, 575-589.
- De Wit, M.J., 1998. On Archean granites, greenstones, cratons and tectonics: does the evidence demand a verdict? *Precambrian Research*, 91, 181-226.
- Davidson, A., 1998. Questions of correlation across the Grenville Front east of Sudbury, Ontario. *Current Research 1998-C*, Geological Survey of Canada, Paper 98-IC, 145-154.
- Dey, S., 2015. Geological history of the Kaladgi–Badami and Bhima basins, south India: sedimentation in Proterozoic intracratonic set-up. In: Mazumder, R., Eriksson, P.G. (eds.). *Precambrian basins of India: stratigraphic and tectonic context*. London, The Geological Society, 43 (1, Memoirs), 283-296.
- Dong, Z., Tang, J., Unsworth, M., Chen, X., 2015. Electrical resistivity structure of the upper mantle beneath Northeastern China: Implications for rheology and the mechanism of craton destruction. *Journal of Asian Earth Sciences*, 100, 115-131. DOI: <https://doi.org/10.1016/j.jseaes.2015.01.008>
- Duba, A., Heikamp, S., Meurer, W., Nover, G., Will, G., 1994. Evidence from borehole samples for the role of accessory minerals in lower-crustal conductivity. *Nature*, 367, 59-61.
- Ducea, M.N., Park, S.K., 2000. Enhanced mantle conductivity from sulfide minerals, southern Sierra Nevada, California. *Geophysical Research Letters*, 27, 2405-2408.

- Duncan, P.M., Hwang, A., Edwards, R.N., Bailey, R., Garland, G.D., 1980. The development and applications of a wide band electromagnetic sounding system using a pseudo-noise source. *Geophysics*, 45, 1276-1296.
- Easton, R.M., 1992. The Grenville Province and the Proterozoic history of Central and Southern Ontario. *Geology of Ontario. Ontario Geological Survey*, 4 (Special volume), 713-904.
- Evans, S., Jones, A.G., Spratt, J., Katsube, J., 2005. Central Baffin electromagnetic experiment (CBEX): Mapping the North American Central Plains (NACP) in the Canadian arctic. *Physics of the Earth and Planetary Interiors*, 150, 107-122.
- Ferguson, I.J., Jones, A.G., Chave, A.D., 2012. Case histories and geological applications. In book *The Magnetotelluric Method: Theory and Practice*, Cambridge University Press, 480-544.
- Fourel, L., Milelli, L., Jaupart, C., Limare, A., 2013. Generation of continental rifts, basins, and swells by lithosphere instabilities. *Journal of Geophysical Research: Solid Earth*, 118, 3080-3100. DOI: <http://dx.doi.org/10.1002/jgrb.50218>
- Glover, P.W.J., Vine, F.J., 1992. Electrical conductivity of carbon bearing granulite at raised temperatures and pressures. *Nature*, 360, 723-726.
- Gokarn, S.G., Rao, C.K., Singh, B.P., Nayak, P.N., 1992. Magnetotelluric studies across the Kurduwadi gravity feature. *Physics of the Earth and Planetary Interiors*, 72(1-2), 58-67. DOI: [https://doi.org/10.1016/0031-9201\(92\)90049-2](https://doi.org/10.1016/0031-9201(92)90049-2)
- Gokarn, S.G., Gupta, G., Rao, C.K., 2004. Geoelectric structure of the Dharwar craton from magnetotelluric studies: Archean suture identified along the Chitradurga-Gadag schist belt. *Geophysical Journal International*, 158, 712-728. DOI: 10.1111/j.1365-246X.2004.02279.x
- Groom, R.W., Bailey, R.C., 1989. Decomposition of magnetotelluric impedance tensors in the presence of local three-dimensional galvanic distortion. *Journal of Geophysical Research*, 94, 1913-1925.
- Gupta, M.L., Sharma, S.R., Sundar, A., 1991. Heat flow and heat generation in the Archaean Dharwar cratons and implications for the Southern Indian shield geotherm and lithospheric thickness. *Tectonophysics*, 194, 107-122. DOI: 10.1016/0040-1951(91)90275-W
- Haak, V., Hutton, R., 1986. *Electrical resistivity in continental lower crust*. London, The Geological Society, 24 (1, Special Publications), 35-49.
- Hasnani, I., Qureshy, M.N., 1971. Palaeomagnetism and Geochemistry of some dykes, Mysore state, India. *Journal of Geophysical Research*, 76, 4786-4795.
- Hegde, V.S., Chavadi, V.C., 2009. Geochemistry of late Archaean meta greywackes from the Western Dharwar Craton, South India: Implications for provenance and nature of the Late Archaean crust. *Gondwana Research*, 15, 178-187.
- Hermance, J.F., 1979. The electrical conductivity of materials containing partial melts: a simple model from Archie's law. *Geophysical Research Letters*, 6, 613-616.
- Hirth, G., Evans, R.L., Chave, A.D., 2000. Comparison of continental and oceanic mantle electrical conductivity: is the Archean lithosphere dry? *Geochemistry Geophysics Geosystems*, 1, 1030. DOI: 10.1029/2000GC000048
- Hyndman, R.D., Shearer, P.M., 1989. Water in the lower continental crust: modelling magnetotelluric and seismic reflection results. *Geophysical Journal International*, 98, 343-365.
- Jayananda, M., Kano, T., Peucat, J.-J., Channabasappa, S., 2008. 3.35 Ga komatiite volcanism in the western Dharwar craton, southern India: Constraints from Nd isotopes and whole-rock geochemistry. *Precambrian Research*, 162, 160-179. DOI: <http://dx.doi.org/10.1016/j.precamres.2007.07.010>
- Jayananda, M., Tsutsumi, Y., Miyazaki, T., Gireesh, R.V., Kapfo, K., Tushipokla, Hidaka, H., Kano, T., 2013. Geochronological constraints on Meso-neoarchean regional metamorphism and magmatism in the Dharwar craton, southern India. *Journal of Asian Earth Sciences*, 78, 18-38. DOI: <http://dx.doi.org/10.1016/j.jseaes.2013.04.033>
- Jayananda, M., Santosh, M., Aadhisesan, K.R., 2018. Formation of Archean (3600–2500 Ma) continental crust in the Dharwar Craton, southern India. *Earth-Science Reviews*, 181, 12-42. DOI: <https://doi.org/10.1016/j.earscirev.2018.03.013>
- Jayaprakash, A.V., 2007. *Puarana Basins of Karnataka*. Kolkata, Geological Survey of India, Memoirs, 129, 136pp.
- Jiracek, G.R., Ander, M.E., Holcombe, H.T., 1979. Magnetotelluric soundings of crustal conductive zones in major continental rifts. In: (eds.) *Rio Grande Rift: Tectonics and Magmatism* edited by Riecker, R. E., American Geophysical Union, Washington, DC, 209-222.
- Jones, A.G., 1981. On a type classification of lower crustal layers under Precambrian regions. *Journal of Geophysics*, 49, 226-233.
- Jones, A.G., 1988. Static shift of magnetotelluric data and its removal in a sedimentary basin environment. *Geophysics*, 53, 967-978. DOI: 10.1190/1.1442533
- Jones, A.G., 1992. Electrical conductivity of the continental lower crust. In: Fountain, D.M., Arculus, R.J., Kay, R.W. (eds.). *Continental Lower Crust*. Amsterdam, Elsevier, 81-143.
- Jones, A.G., 1993. The COPROD2 dataset: Tectonic setting, Recorded MT Data, and Comparison of models. *Journal of Geomagnetism and Geoelectricity*, 45(9), 933-955. DOI: 10.5636/jgg.45.933
- Jones, A.G., 1999. Imaging the continental upper mantle using electromagnetic methods. *Lithos*, 48, 57-80.
- Jones, A.G., Ledo, J., Ferguson, I.J., 2005. Electromagnetic images of the Trans-Hudson orogen: the North American Central Plains (NACP) anomaly revealed. *Canadian Journal of Earth Sciences*, 42, 457-478.
- Julia, J., Jagadeesh, S., Rai, S.S., Owens, T.J., 2009. Deep crustal structure of the Indian Shield from joint inversion of P-wave receiver functions and Rayleigh-wave group velocities: implications for Precambrian evolution. *Journal of Geophysical Research*, 11, 4. DOI: <http://dx.doi.org/10.1029/2008JB006261>
- Kaila, K.L., Roy Chowdhury, K., Reddy, P.R., Krishna, V.G., Narain, H., Subbotin, S.I., Sollogub, V.B., Chekunov, A.V., Kharetechko, G.E., Lazarenko, M.A., Ilchenko, T.V., 1979. Crustal structure

- along Kavali-Udipi profile in the Indian peninsular shield from Deep Seismic Sounding. *Journal of Geological Society of India*, 20, 307-333.
- Karato, S., 1990. The role of hydrogen in the electrical conductivity of the upper mantle. *Nature*, 347, 272-273.
- Kariya, K.A., Shankland, T.J., 1983. Electrical conductivity of dry lower crustal rocks. *Geophysics*, 48, 52-61.
- Keller, G.V., 1989b. Electrical structure of the crust and upper mantle beneath the United States: Part 2, Survey of data and interpretation. In: Pakiser, L., Mooney, W.D. (eds.). *Geophysical Framework of the Continental United States. Memoir of the Geological Society of America*, 172, 425-446.
- Khoza, D., Jones, A.G., Muller, M.R., Evans, R.L., Webb, S.J., Miensoopust, M., the SAMTEX team, 2013. Tectonic model of the Limpopo belt: Constraints from magnetotelluric data. *Precambrian Research*, 226, 143-156.
- Klein, G.D., 1995. Intracratonic basins. In: Busby, C.J., Ingersoll, R.V. (eds.). *Tectonics of Sedimentary Basins. Malden (MA), Blackwell Science*, 459-478.
- Korja, T., Hjelt, S-E., 1993. Electromagnetic studies in the Fennoscandian Shield-electrical conductivity of Precambrian crust. *Physics of the Earth and Planetary Interiors*, 81(1), 107-138.
- Korja, T., 2007. How is the European lithosphere imaged by magnetotellurics? *Surveys in Geophysics*, 28, 239-272.
- Kumar, A., Bhaskar Rao, Y.J., Sivaraman, T.V., Gopalan, K., 1996. Sm-Nd ages of Archaean metavolcanics of the Dharwar craton, South India. *Precambrian Research*, 80, 205-216.
- Kumar, N., Zeyen, H., Singh, A.P., Singh, B., 2013. Lithospheric structure of Southern Indian shield and adjoining oceans: integrated modelling of topography, gravity, geoid and heat flow data. *Geophysical Journal International*, 194, 30-44.
- Kusham, Pratap, A., Pradeep Naick, B., Naganjaneyulu, K., 2018. Lithospheric architecture in the Archaean Dharwar craton, India: a magnetotelluric model. *Journal of Asian Earth Sciences*, 163, 43-53.
- Kusham, Pratap, A., Pradeep Naick, B., Naganjaneyulu, K., 2019. Crustal and Lithospheric mantle conductivity structure in the Dharwar craton, India. *Journal of Asian Earth Sciences*, 176, 253-263.
- Kusham, Pradeep Naick, B., Pratap, A., Naganjaneyulu, K., 2021a. Magnetotelluric 3-D full tensor inversion in the Dharwar craton, India: Mapping of subduction polarity and kimberlitic melt. *Physics of the Earth and Planetary Interiors*, 315, 106708. DOI: <https://doi.org/10.1016/j.pepi.2021.106708>
- Kusham, Pradeep Naick, B., Pratap, A., Naganjaneyulu, K., 2021b. 2-D versus 3-D Magnetotelluric Data Interpretation: A case study from the Dharwar craton, India. *Tectonophysics*, 816, 229028. DOI: <https://doi.org/10.1016/j.tecto.2021.229028>
- Krishna Brahmam, N., Negi, J.G., 1973. Rift valleys beneath Deccan Traps (India). *Geophysical Research Bulletin*, 11, 207-237.
- Krishnamurthy, P., 2020. The Deccan Volcanic Province (DVP), India: A Review. *Journal of the Geological Society of India*, 96, 9-35. DOI: <https://doi.org/10.1007/s12594-020-1501-5>
- McNeice, G.W., Jones, A.G., 2001. Multisite, multifrequency tensor decomposition of magnetotelluric data. *Geophysics*, 66, 158-173.
- Miall, A.D. 1984. *Principles of Sedimentary Basin Analysis*. New York, Springer, 490pp.
- Mibe, K., Fujii, T., Yasuda, A., 1998. Connectivity of aqueous fluid in the Earth's upper mantle. *Geophysical Research Letters*, 25, 1233-1236.
- Miensoopust, M., Jones, A.G., Muller, M.R., Garcia, X., Evans, R.L., 2011. Lithospheric structures and Precambrian terrane boundaries in northeastern Botswana revealed through magnetotelluric profiling as part of the Southern African Magnetotelluric Experiment. *Journal of Geophysical Research: Solid Earth*, 116, B02401.
- Muller, M.R., Jones, A.G., Evans, R.L., Grutter, H.S., Hatton, C., Garcia, X., Hamilton, M.P., Miensoopust, M.P., Cole, P., Ngwisanyi, T., Hutchins, D., Fourie, C.J., Jelsma, H.A., Evans, S.F., Aravanis, T., Pettit, W., Webb, S.J., Wasborg, J., The SAMTEX Team, 2009. Lithospheric structure, evolution and diamond prospectivity of the Rehoboth Terrane and the western Kaapvaal Craton, southern Africa: constraints from broadband magnetotellurics. *Lithos*, 112S, 93-105.
- Naganjaneyulu, K., 2010. Granitic and magmatic bodies in the deep crust of the Son Narmada Region, Central India: constraints from seismic, gravity and magnetotelluric methods. *Earth Planets Space*, 62, 863-868.
- Naganjaneyulu, K., Harinarayana, T., 2004. Deep crustal electrical signatures of eastern Dharwar craton, India. *Gondwana Research*, 7, 951-960.
- Naganjaneyulu, K., Santosh, M., 2010a. The Cambrian collisional suture of Gondwana in southern India: A geophysical appraisal. *Journal of Geodynamics*, 50, 256-267. DOI: [10.1016/j.jog.2009.12.001](https://doi.org/10.1016/j.jog.2009.12.001)
- Naganjaneyulu, K., Santosh, M., 2010b. The Central India Tectonic Zone: a geophysical perspective on continental amalgamation along a Mesoproterozoic suture. *Gondwana Research*, 18, 547-564. DOI: [10.1016/j.gr.2010.02.017](https://doi.org/10.1016/j.gr.2010.02.017)
- Naganjaneyulu, K., Santosh, M., 2011. Crustal architecture beneath Madurai Block, southern India deduced from magnetotelluric studies: implications for subduction-accretion tectonics associated with Gondwana assembly. *Journal of Asian Earth Sciences*, 40, 132-143.
- Naganjaneyulu, K., Santosh, M., 2012. The nature and thickness of lithosphere beneath the Archean Dharwar Craton, southern India: A magnetotelluric model. *Journal of Asian Earth Sciences*, 49, 349-361. DOI: [10.1016/j.jseae.2011.07.002](https://doi.org/10.1016/j.jseae.2011.07.002)
- Nagarjuna, D., Rao, C.K., Kumar, A., 2017. Geoelectric structure of northern Cambay rift basin from magnetotelluric data. *Earth, Planets and Space*, 69, 140. DOI: <https://doi.org/10.1186/s40623-017-0725-0>
- Naqvi, S.M., Rogers, J.J.W., 1987. *Precambrian Geology of India*. Oxford, Oxford University Press, 223pp.
- Negi, J.G., Pandey, O.P., Agrawal, P.K., 1986. Super-mobility of hot Indian lithosphere. *Tectonophysics*, 131, 147-156.
- Newton, R.C., 1990. Fluids and melting in the Archean deep crust of S. India. In: Ashworth, J.R., Brown, M. (eds.). *High*

- Temperature Metamorphism and Crustal Anatexis. London, Unwin Hyman, 160-179.
- Pape, F.L., Jones, A.G., Jessell, M.W., Perrouty, S., Gallardo, L.A., Baratoux, L., Hogg, C., Siebenaller, L., Touré, A., Ouyi, P., Boren, G., 2017. Crustal structure of southern Burkina Faso inferred from magnetotelluric, gravity and magnetic data. *Precambrian Research*, 300, 261-272. DOI: <https://doi.org/10.1016/j.precamres.2017.08.013>
- Peucat, J.J., Bouhallier, H., Fanning, C.M., Jayananda, M., 1995. Age of the Holenarsipur Greenstone Belt, Relationships with the Surrounding Gneisses (Karnataka, south India). *The Journal of Geology*, 103, 701-710.
- Pina-Varas, P., Ledo, J., Queralt, P., Marcuello, A., Bellmunt, F., Hidalgo, R., Messeiller, M., 2014. 3-D Magnetotelluric exploration of Tenerife Geothermal System (Canary Islands, Spain). *Surveys in Geophysics*, 35, 1045-1064. DOI: 10.1007/s10712-014-9280-4
- Pratap, A., Kusham, Pradeep Naick, B., Naganjaneyulu, K., 2018. A magnetotelluric study from over Dharwar cratonic nucleus into Billigiri Rangan charnockitic massif, India. *Physics of the Earth and Planetary Interiors*, 280, 32-39.
- Raase, P., Raith, M., Ackermann, D., Lal, R.K., 1986. Progressive Metamorphism of Mafic Rocks from Greenschist to Granulite Facies in the Dharwar Craton of South India. *The Journal of Geology*, 94, 261-282.
- Radhakrishna, B.P., Naqvi, S.M., 1986. Precambrian continental crusts of India and its evolution. *The Journal of Geology*, 94, 145-166.
- Rai, S.S., Priestly, K., Suryaprakasam, K., Srinagesh, D., Gaur, V.K., Du, Z., 2003. Crustal shear velocity structure of the South India shield. *Journal of Geophysical Research*, 108, B2, 2088. DOI: 10.1029/2002JB001776
- Rajaram, M., Anand, S.P., 2003. Crustal Structure of South India From Aeromagnetic Data. *Journal of the Virtual Explorer*, 12, 72-82.
- Ramakrishna, T.S., Chayanulu, A.Y.S.R., 1988. A geophysical appraisal of the Purana basins of India. *Journal of the Geological Society of India*, 32, 48-60.
- Ramakrishnan, M., Vaidyanadhan, R., 2010. *Geology of India*. Bangalore, Geological Society of India, 1, 556pp.
- Rao, C.K., Singh, B.P., 1995. Upper Crustal Structure in the Tomi-Purnad Region, Central India, Using Magnetotelluric Studies. *Journal of geomagnetism and geoelectricity*, 47(4), 411-420.
- Rao, C.K., Selvaraj, C., Gokarn, S.G., 2014. Deep electrical structure over the igneous arc of the Indo Burman Orogen in Sagaing province, Myanmar from magnetotelluric studies. *Journal of Asian Earth Sciences*, 94, 68-76. DOI: <https://doi.org/10.1016/j.jseaes.2014.08.016>
- Ravi Kumar, M., Saul, J., Sarkar, D., Kind, R., Anshu, K., Shukla, A.K., 2001. Crustal structure of the India Shield: New constraints from teleseismic receiver functions. *Geophysical Research Letters* 28, 1339-1342.
- Rodi, W., Mackie, R.L., 2001. Nonlinear conjugate gradients algorithm for 2-D magnetotelluric inversion. *Geophysics*, 66, 174-187.
- Rodi, W., Mackie, R.L., 2012. The inverse problem. In: Chave, A.D., Jones, A.G. (eds.). *The Magnetotelluric Method: Theory and Practice*. New York, Cambridge University Press, 347-414.
- Roy, S., Rao, R.U.M., 2000. Heat flow in the Indian shield. *Journal of Geophysical Research*, 105(B11), 25,587-25,604. DOI: 10.1029/2000JB900257
- Roy, S., Ray, L., Bhattacharya, A., Srinivasan, R., 2008. Heat flow and crustal thermal structure in the Late Archaean Closepet Granite batholith, south India. *International Journal of Earth Sciences, Geologische Rundschau* 97, 245-256. DOI: 10.1007/s00531-007-0239-2
- Saikia, U., Das, R., Rai, S.S., 2017. Possible magmatic underplating beneath the west coast of India and adjoining Dharwar craton: imprint from Archean crustal evolution to breakup of India and Madagascar. *Earth and Planetary Science Letters*, 462, 1-17.
- Sarafian, E., Evans, R.L., Abdelsalam, M.G., Atekwana, E., Elsenbeck, J., Jones, A.G., Chikambwe, E., 2018. Imaging Precambrian lithospheric structure in Zambia using electromagnetic methods. *Gondwana Research*, 54, 38-49. DOI: 10.1016/j.gr.2017.09.007
- Sarkar, D., Chandrakala, K., Padmavathi Devi, P., Sridhar, A.R., Sain, K., Reddy, P.R., 2001. Crustal velocity structure of western Dharwar craton, south India. *Journal of Geodynamics*, 31, 227-241.
- Schilling, F.R., Partzsch, G.M., Brasse, H., Schwarz, G., 1997. Partial melting below the magmatic arc in the central Andes deduced from geoelectromagnetic field experiments and laboratory data. *Physics of the Earth and Planetary Interiors* 103, 17-31.
- Schwarz, G., 1990. Electrical conductivity of the Earth's crust and upper mantle. *Surveys in Geophysics*, 11, 133-161.
- Selway, K., Hand, M., Payne, J.L., Heinson, G.S., Reid, A., 2011. Magnetotelluric constraints on the tectonic setting of Grenville-aged orogenesis in central Australia. *Journal of the Geological Society*, 168(1), 251-264. DOI: 10.1144/0016-76492010-034
- Selway, K., 2014. On the causes of electrical conductivity anomalies in tectonically stable lithosphere. *Surveys in Geophysics*, 35, 219-257.
- Srinivasan, R., Naha, K., 1993. Archaean sedimentation in the Dharwar craton, southern India. *Proceedings of the National Academy of Sciences, India*, 63(A), 1-13.
- Subrahmanyam, C., Verma, R.K., 1982. Gravity interpretation of the Dharwar greenstonegneiss-granite terrain in the southern Indian shield and its geological implications. *Tectonophysics*, 84, 225-245.
- Swami Nath, J., Ramakrishnan, M., 1981. Early Precambrian Supracrustals of Southern Karnataka. *Geological Survey of India*, 112 (Memoir), 351pp.
- Taylor, P.N., Chadwick, B., Moorbath, S., Ramakrishnan, M., Viswanatha, M.N., 1984. Petrography, chemistry and isotopic ages of Peninsular Gneiss, Dharwar acid volcanic rocks and the Chitradurga granite with special reference to the late Archaean evolution of the Karnataka craton. *Precambrian Research*, 23, 349-375.

- Wannamaker, P.E. 1997. Comment on “The petrologic case for a dry lower crust” by B.W.D. Yardley and J.W. Valley. *Journal of Geophysical Research*, 102, 12173-12185.
- White, R., McKenzie, D., 1989. Magmatism at rift zones: The generation of volcanic continental margins and flood basalts. *Journal of Geophysical Research*, 94, 7685-7729.
- Wu, X., Ferguson, I. J., Jones, A.G., 2002. Magnetotelluric response and geoelectric structure of the Great Slave Lake shear zone. *Earth and Planetary Science Letters*, 196, 35-50.
- Yardley, B.W.D., Valley, J.W., 1997. The petrologic case for a dry lower crust. *Journal of Geophysical Research*, 102, 12172-12185.
- Yellappa, T., Santosh, M., Chetty, T.R.K., Kwon, S., Park, C., Nagesh, P., Mohanty, D.P., Venkatasivappa, V., 2012. A Neoproterozoic dismembered ophiolite complex from southern India: geochemical and geochronological constraints on its suprasubduction origin. *Gondwana Research*, 21, 246-265.
- Yoshino, T., Manthilake, G., Matsuzaki, T., Katsura, T., 2008. Dry mantle transition zone inferred from the conductivity of wadsleyite and ringwoodite. *Nature*, 451, 326-329.

**Manuscript received April 2022;  
revision accepted January 2023;  
published Online March 2023.**